BOTULISM

Delivery of single-domain antibodies into neurons using a chimeric toxin–based platform is therapeutic in mouse models of botulism

Shin-Ichiro Miyashita[1,2], Jie Zhang[1,2], Sicai Zhang[1,2], Charles B. Shoemaker[3], Min Dong[1,2]*

Efficient penetration of cell membranes and specific targeting of a cell type represent major challenges for developing therapeutics toward intracellular targets. One example facing these hurdles is to develop post-exposure treatment for botulinum neurotoxins (BoNTs), a group of bacterial toxins (BoNT/A to BoNT/G) that are major potential bioterrorism agents. BoNTs enter motor neurons, block neurotransmitter release, and cause a paralytic disease botulism. Members of BoNTs such as BoNT/A exhibit extremely long half-life within neurons, resulting in persistent paralysis for months, yet there are no therapeutics that can inhibit BoNTs once they enter neurons. Here, we developed a chimeric toxin–based delivery platform by fusing the receptor-binding domain of a BoNT, which targets neurons, with the membrane translocation domain and inactivated protease domain of the recently discovered BoNT-like toxin BoNT/X, which can deliver cargoes across endosomal membranes into the cytosol. A therapeutic protein was then created by fusing a single-domain antibody (nanobody) against BoNT/A with the delivery platform. In vitro characterization demonstrated that nanobodies were delivered into cultured neurons and neutralized BoNT/A in neurons. Administration of this protein in mice shortened duration of local muscle paralysis, restoring muscle function within hours, and rescued mice from systemic toxicity of lethal doses of BoNT/A. Fusion of two nanobodies, one against BoNT/A and the other against BoNT/B, created a multivalent therapeutic protein able to neutralize both BoNT/A and BoNT/B in mice. These studies provide an effective post-exposure treatment for botulism and establish a platform for intracellular delivery of therapeutics targeting cytosolic proteins and processes.

INTRODUCTION

Botulinum neurotoxins (BoNTs) are a family of bacterial toxins with seven major serotypes (BoNT/A to BoNT/G) (*1*–*6*). They are the most potent toxins known and classified in the United States as one of the six most dangerous potential bioterrorism agents (category A and tier 1) (*7*). These toxins target and enter motor neurons and block neurotransmitter release, causing the disease known as botulism, whose defining symptom is flaccid paralysis (losing the ability to contract muscles). Among the seven serotypes, BoNT/A, BoNT/B, and BoNT/E (and rarely BoNT/F) are associated with human botulism, with BoNT/A and BoNT/B responsible for most cases. Although rare, botulism cases persist in human populations with a death rate of ~3 to 5% (*8*, *9*).

A major challenge for addressing the threats posed by BoNT/A and BoNT/B is their extraordinarily long half-life within the cytosol of neurons (*10*–*14*), leading to persistent nerve blockade and muscle paralysis that lasts for months in humans. Patients must rely on intensive care and mechanical ventilation for weeks to months to stay alive, which renders the treatment expensive and could easily overwhelm the health care system during a large-scale outbreak (*7*).

BoNT/A and BoNT/B are also the two serotypes approved for treating a multitude of medical conditions as well as for reducing wrinkles, benefiting millions of people every year (*1*, *2*, *15*). BoNT/A is the dominant form in clinical use. Local injection of tiny amounts of BoNT/A provides persistent muscle relaxation that lasts 4 to 6 months. However, if the patient is dissatisfied with the effect or there is unwanted diffusion of BoNT/A, there are no available post-exposure remedies that can reverse paralysis.

BoNTs are composed of two chains and three functional domains: a light chain (LC; ~50 kDa), which is a protease domain, and a heavy chain (HC), which can be further divided into a membrane translocation domain (H_N, ~50 kDa) and a receptor-binding domain (H_C,~50 kDa). BoNTs are initially synthesized as a single polypeptide. The linker region between LC and HC needs to be proteolytically cleaved to generate the active di-chain form, in which the LC remains covalently connected to the HC via an interchain disulfide bond (*1*, *2*, *4*). These toxins target motor neurons with extraordinary specificity by binding to neuronal receptors through the H_C and enter neurons via receptor-mediated endocytosis (*1*, *5*). A drop in pH within endosomes then triggers conformational changes in the H_N, leading to translocation of the LC across endosomal membranes into the cytosol (*1*, *2*, *4*, *16*–*19*). The interchain disulfide bond is reduced once the LC reaches the cytosol, thus releasing the LC (*16*, *20*). The LC then cleaves a specific set of neuronal proteins belonging to the SNARE (soluble *N*-ethylmaleimide–sensitive factor attachment protein receptor) protein family, including synaptosomal-associated protein of 25 kDa (SNAP-25; cleaved by BoNT/A, BoNT/E, and BoNT/C), syntaxin 1 (cleaved by BoNT/C), and three homologous vesicle membrane proteins, vesicle-associated membrane protein (VAMP) 1, 2, and 3 (cleaved by BoNT/B, BoNT/D, BoNT/F, and BoNT/G) (*1*, *2*, *4*, *21*). Syntaxin 1 and SNAP-25 are localized on plasma membranes and form a complex with VAMPs, known as the SNARE complex, which is the core machinery mediating fusion of synaptic vesicle membranes to the plasma membranes (*22*, *23*). Cleavage of any one of these three SNARE

[1]Department of Urology, Boston Children's Hospital, Boston, MA 02115, USA. [2]Department of Surgery and Department of Microbiology, Harvard Medical School, Boston, MA 02115, USA. [3]Department of Infectious Diseases and Global Health, Cummings School of Veterinary Medicine at Tufts University, North Grafton, MA 01536, USA.
*Corresponding author. Email: min.dong@childrens.harvard.edu

proteins disrupts vesicle membrane fusion to plasma membranes, thus blocking the release of neurotransmitters (*2*, *21*, *22*).

It has been shown that the LC of BoNT/A (LC/A) maintains its activity within neurons for months, which is the reason for its ability to induce persistent paralysis that lasts 4 to 6 months in humans (*10*–*14*). Intoxicated neurons fully recover their function once the toxin LC loses its activity. Thus, successful treatment of botulism requires targeting and inhibiting LCs within neurons. However, there are no small-molecule inhibitors that work effectively in neurons (*24*, *25*). BoNT-neutralizing antibodies have been developed (*26*–*29*), but they are useful only before toxins enter neurons.

Because BoNTs are capable of targeting motor neurons and delivering their LCs into neurons, they potentially can serve as carriers to deliver cargoes into neurons. Bade *et al.* (*30*) previously tested this possibility by fusing different proteins to the N terminus of the full-length active form of BoNT/D and examined their delivery on cultured neurons, using cleavage of VAMP2 by BoNT/D-LC (LC/D) in neurons as a sensitive readout for successful delivery into the cytosol. They found that fusion of a dihydrofolate reductase (DHFR) or an LC/A did not affect overall translocation efficacy, whereas fusion of firefly luciferase or green fluorescent protein (GFP) reduced translocation efficacy. These findings demonstrate that a protein cargo can be delivered into the cytosol of neurons through direct fusion to a BoNT, and the translocation efficacy varies depending on cargo proteins.

To be used as a delivery tool, BoNTs must first be "detoxified," which has been proven to be challenging. Simply deleting the LC often creates solubility issues due to disrupting native interactions between LC and H_N (*31*–*33*). An alternative approach is to abolish LC protease activity by mutating key residues. LCs are zinc-dependent proteases with a conserved HEXXH motif (*34*, *35*). Mutations are usually introduced to one or two residues in this motif plus two residues that are conserved in all BoNTs and critical for their protease activity (R363A and Y366F in BoNT/A) (*36*). Catalytically inactive forms of BoNT/A and BoNT/C containing three designed point mutations have been developed and shown to have no protease activity. However, both still induced flaccid paralysis and death in mice with median lethal doses (LD_{50}) of ~0.5 to 5 mg/kg (intraperitoneal injection) (*37*–*39*). This residual toxicity has been independently reported for catalytically inactive full-length BoNT/A, BoNT/B, BoNT/C, BoNT/E, and BoNT/F containing three point mutations in their LCs (*40*). The source of this residual toxicity remains unknown, and it could be due to the translocation process. Although this toxicity is far lower compared with active toxins (0.1 to 5 ng/kg intraperitoneal injection LD_{50} in mice) (*41*), it is a major safety barrier to the development of BoNTs as delivery tools.

We recently identified a BoNT-like toxin, termed BoNT/X (*42*). It has not only the same conserved domain structure as other BoNTs but also a few distinct features. For instance, the LC of BoNT/X (LC/X) cleaves not only the canonical substrates VAMP1/2/3 but also additional VAMP family members VAMP4, VAMP5, and Ykt6 (*42*). Furthermore, the H_C of BoNT/X (H_C/X) does not target motor neurons in mice, and the host species targeted by BoNT/X remains to be established. The fragment containing the LCH_N of BoNT/X (LCH_N/X) can translocate its LC more efficiently into neurons than the corresponding fragments of BoNT/A and BoNT/B (*42*). Using LCH_N/X, here, we developed a chimeric toxin–based delivery platform by deactivating its protease activity and fusing it to the H_C of a BoNT. Therapeutic proteins targeting BoNT-LCs were then created by fusion of the chimeric inactive toxin platform with LC-specific single-domain antibodies (known as VHHs or nanobodies), which are ~12- to 15-kDa proteins derived from the single variable domain of the HC-only antibodies in *Camelidae* such as alpacas and llamas. Such therapeutic proteins showed no toxicity at doses of up to 100 mg/kg in vivo in mice and successfully neutralized BoNT-LC activity in neurons, shortened the duration of muscle paralysis, and rescued mice from lethal doses of BoNT/A and BoNT/B after the onset of botulism.

RESULTS

Chimeric inactive toxin-based delivery platform shows no toxicity in vivo

To explore whether LCH_N/X can be used to construct a delivery tool, we created three detoxified chimeric toxins by (i) fusing LCH_N/X with the H_C of BoNT/A (H_C/A), BoNT/C (H_C/C), or BoNT/D (H_C/D) (these H_Cs essentially replace H_C/X and confer specificity toward mammalian motor neurons) (Fig. 1, A and B, and fig. S1A), (ii) introducing three point mutations (E228Q/R360A/Y363F) in LC/X to abolish its protease activity (designated catalytically inactive form, $^{ci}LCH_N$), and (iii) modifying the linker region between the LC and H_N to include a thrombin cleavage site, which enables us to specifically convert the chimeric toxin from a single chain into a di-chain form using thrombin. In addition, a thrombin cleavage site was also introduced before the C-terminal His6 tag to cleave off the His6 tag after protein purification.

These catalytically inactive toxins were termed ^{ci}BoNT/XA, ^{ci}BoNT/XC, and ^{ci}BoNT/XD. We then selected a previously reported nanobody (known as VHH-ALc-B8, abbreviated "A8" here), which was raised against recombinantly purified LC/A in alpaca and has been demonstrated to inhibit LC/A in vitro and in cells (*43*, *44*). A8 served as a cargo and was fused directly to the N terminus of chimeric toxins, generating A8-^{ci}BoNT/XA (Fig. 1, A and B), A8-^{ci}BoNT/XC, and A8-^{ci}BoNT/XD (fig. S1A). For comparison, we also constructed a catalytically inactive form of BoNT/C (^{ci}BoNT/C) containing the same set of three point mutations in its LC as in ^{ci}LC/X as well as A8-^{ci}BoNT/C fusion protein (fig. S1B).

These fusion proteins were expressed and purified in *Escherichia coli* and readily converted into a di-chain form by thrombin treatment (fig. S1, C and D). The interchain disulfide bond was formed as the reducing agent dithiothreitol (DTT) separated these proteins into two parts: one is ^{ci}LC (~50 kDa) or A8-^{ci}LC (~65 kDa) and the other is H_N-H_C (~100 kDa; fig. S1, C and D). A8-^{ci}BoNT/XA showed similar potency as A8 alone in inhibiting LC/A activity in vitro (fig. S1E).

We first examined whether these fusion proteins have any toxicity in vivo in mice. Intraperitoneal injection of A8-^{ci}BoNT/C caused death of five of six mice at 0.8 mg/kg (table S1). Injection of A8 alone or boiled A8-^{ci}BoNT/C caused no death, whereas ^{ci}BoNT/C alone induced death at 2 mg/kg range (table S1). These findings are consistent with previous reports that BoNTs with inactive LCs still show residual toxicity (*37*, *40*). In contrast, mice injected with A8-^{ci}BoNT/XA, A8-^{ci}BoNT/XC, or A8-^{ci}BoNT/XD at 100 mg/kg did not show any paralysis, and no death occurred (table S1).

A8-^{ci}LC/X is delivered into the cytosol of cultured neurons

We next analyzed whether the chimeric inactive toxin platform can deliver the A8-^{ci}LC/X fragment into the cytosol of cultured neurons. The experimental design took advantage of the fact that A8-^{ci}LC/X

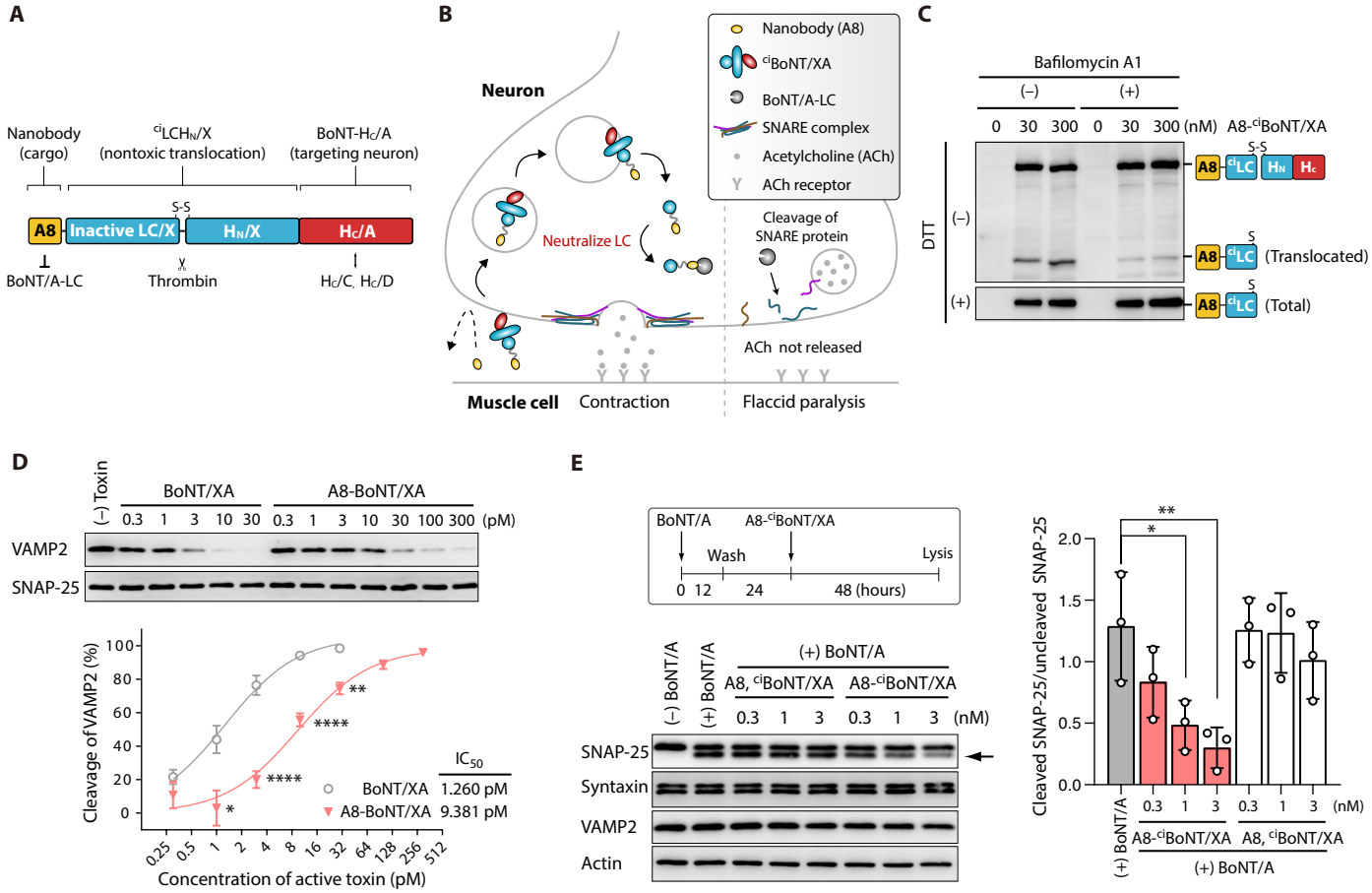

Fig. 1. A chimeric inactive toxin ^{ci}BoNT/XA delivered the fused nanobody against LC/A into neurons. (**A**) Schematic drawing of the A8-^{ci}BoNT/XA fusion protein. ^{ci}LCH$_N$/X is fused with a BoNT-H$_C$ (H$_C$/A, H$_C$/C, or H$_C$/D). LC/X is deactivated by three point mutations. The linker region between ^{ci}LC/X and H$_N$/X is modified to include a thrombin cleavage site. A8: VHH-ALc-B8, a nanobody that neutralizes LC/A. (**B**) Schematic illustration of delivering nanobodies via fusion with ^{ci}BoNT/XA to neutralize LC/A in neurons. LC/A cleaves SNAP-25 in neurons, thus blocking fusion of synaptic vesicles to plasma membranes, which is essential for neurotransmitter release. Nanobodies such as A8 cannot enter neurons by themselves. When fused with ^{ci}BoNT/XA, A8-^{ci}BoNT/XA targets and enters neurons via receptor-mediated endocytosis, followed with translocation of A8-^{ci}LC/X into the cytosol. A8-^{ci}LC/X then binds to and inhibits LC/A in neurons. (**C**) Cultured neurons were exposed to A8-^{ci}BoNT/XA for 12 hours with or without bafilomycin A1. Neuron lysates were analyzed by immunoblot analysis under nonreducing conditions. A8 was detected using a goat anti-llama antibody. Cell lysates were also analyzed in the presence of DTT, which reduces the interchain disulfide bond between A8-^{ci}LC and H$_N$-H$_C$, serving as a control. (**D**) Active forms of BoNT/XA and A8-BoNT/XA were generated via sortase-mediated ligation. Cultured neurons were exposed to these toxins, and cleavage of VAMP2 was analyzed by immunoblot. SNAP-25 served as a loading control. Representative blots (one of two to five independent experiments) and quantification of dose-dependent VAMP2 cleavage are shown. Data were analyzed by unpaired two-tailed *t* test; $^*P < 0.05$, $^{**}P < 0.01$, and $^{****}P < 0.0001$. IC$_{50}$, median inhibitory concentration. (**E**) Cultured rat cortical neurons were first exposed to BoNT/A (20 pM, 12 hours), washed, further incubated in toxin-free medium for 24 hours, and then exposed to the indicated concentrations of either A8-^{ci}BoNT/XA or the control mixture of A8 and ^{ci}BoNT/XA proteins for 48 hours. Cell lysates were analyzed by immunoblot to detect SNAP-25, syntaxin 1, and VAMP2. Actin served as a loading control. Representative blots (one of three independent experiments) and quantification of SNAP-25 cleavage are shown. Data were analyzed by one-way ANOVA with Dunnett's post hoc tests; $^*P < 0.05$ and $^{**}P < 0.01$.

is connected via a disulfide bond to the H$_N$-H$_C$ and this disulfide bond is reduced when A8-^{ci}LC/X reaches the cytosol, assisted by the thioredoxin reductase–thioredoxin protein disulfide-reducing system (*16*). If the translocation is not successful, A8-^{ci}LC/X would remain connected with the H$_N$-H$_C$. Thus, the appearance of isolated A8-^{ci}LC/X in neurons indicates successful translocation.

We exposed cultured rat cortical neurons to A8-^{ci}BoNT/XA at 30 and 300 nM concentrations for 12 hours. Neuron lysates were harvested and subjected to immunoblot analysis under nonreducing conditions. An isolated A8-^{ci}LC/X band was clearly detected in neuron lysates (Fig. 1C). To further demonstrate that the A8-^{ci}LC/X bands were generated by translocation across endosomal membranes, we carried out the same experiment in the presence of bafilomycin A1, a small-molecule inhibitor that blocks acidification of endosomes. This treatment did not affect the overall binding of A8-^{ci}BoNT/XA to neurons, because the full-length band at ~165 kDa showed intensity similar to that of neurons not treated with bafilomycin A1, yet bafilomycin treatment reduced the isolated A8-^{ci}LC/X band (Fig. 1C and fig. S2, A to C). Together, these experiments suggest that A8-^{ci}LC/X in A8-^{ci}BoNT/XA can be delivered successfully into the cytosol of cultured rat cortical neurons in vitro.

Delivered A8 and LC/X are functional in the cytosol of neurons

To further estimate the translocation efficacy and determine whether translocated proteins are functional in cells, we built a construct

that expresses A8 fused with the active LCH_N/X containing no mutations in its LC. An additional short sortase recognition tag (residues LPETGG) was added to the C terminus. This tag can be recognized by the bacterial transpeptidase sortase, which can ligate the fusion protein covalently to the N terminus of a second protein containing a free glycine on the N terminus (fig. S3A) (*42*, *45*). We ligated A8-LCH_N/X with the H_C/A, yielding an A8 fused with an active full-length BoNT/XA (termed A8-BoNT/XA; fig. S3, A and B). As a control, we also generated the active BoNT/XA by ligating LCH_N/X and H_C/A (fig. S3B). This approach allowed us to produce limited amounts of active toxin without creating the coding sequence for full-length toxins. A8-BoNT/XA allowed us to examine whether the translocated A8-LC/X was functional in cultured neurons by analyzing cleavage of VAMP2. As shown in Fig. 1D, incubation of cultured neurons with picomolar A8-BoNT/XA or BoNT/XA both resulted in cleavage of VAMP2, demonstrating that the LC in A8-LC is fully functional after translocation. Compared with BoNT/XA, A8-BoNT/XA showed ~7.4-fold reduction in efficacy based on assessing VAMP2 cleavage in neurons (Fig. 1D). A8-LCH_N/X and LCH_N/X showed similar activity in cleaving recombinant VAMP2 protein in vitro, indicating that fusion with A8 does not affect LC activity (fig. S3C). Together, these data suggest that A8-LC/X was delivered into neurons at ~7.4-fold lower efficacy compared with LC/X.

We next evaluated whether the delivered A8-^{ci}LC/X can neutralize LC/A within cultured neurons. Neurons were first exposed to BoNT/A for 12 hours, washed, and further incubated in toxin-free medium for another 24 hours, followed by incubation with A8-^{ci}BoNT/XA for 48 hours (Fig. 1E). Incubation with a mixture of separated A8 and ^{ci}BoNT/XA proteins was analyzed in parallel as a control. Cell lysates were harvested and analyzed by immunoblot, revealing persistent cleavage of SNAP-25 by LC/A (*46*, *47*). Incubation with separated A8 and ^{ci}BoNT/XA did not affect cleavage of SNAP-25, whereas incubation with A8-^{ci}BoNT/XA reduced SNAP-25 cleavage in neurons (Fig. 1E). Similarly, incubation with A8-^{ci}BoNT/XC or A8-^{ci}BoNT/XD also reduced SNAP-25 cleavage in neurons in this post-exposure model (fig. S4). These data demonstrate that ^{ci}BoNT/XA, ^{ci}BoNT/XC, and ^{ci}BoNT/XD were able to deliver a functional A8 into the cytosol of neurons.

We also validated the receptor-binding property of A8-^{ci}BoNT/XA and confirmed that its binding to neurons was reduced by a recombinant protein containing the fourth luminal domain fragment of SV2C, which is a protein receptor for BoNT/A (fig. S5A) (*48*, *49*). Consistently, premixing nanomolar ^{ci}BoNT/XA with picomolar BoNT/A and adding them together to cultured neurons reduced cleavage of SNAP-25 compared with BoNT/A alone, further suggesting that ^{ci}BoNT/XA uses the same receptors as BoNT/A (fig. S5B).

Intramuscular injection of A8-^{ci}BoNT/XA shortens BoNT/A-induced leg muscle paralysis

To next assess A8-^{ci}BoNT/XA in vivo, we used a local paralysis model known as the Digit Abduction Score (DAS) assay (*50*). Sublethal doses of BoNT/A are injected intramuscularly into the hind legs of mice, which paralyzes the leg muscle and prevents toe spreading during the startle response. The degree of toe spreading is scored 0 to 4 (Fig. 2A). Injection of BoNT/A at 6 pg induced the severest scores of 3 to 4. In mice, possibly due to their fast metabolism rates, BoNT/A induces paralysis that lasts ~30 to 40 days (Fig. 2B). To develop a post-exposure model, we first injected BoNT/A and waited 18 hours, by which time the leg is already paralyzed with scores 2 to 3. We then carried out an intramuscular injection of A8-^{ci}BoNT/XA to the same BoNT/A injection site (Fig. 2B). Separated A8 and ^{ci}BoNT/XA proteins were analyzed in parallel as controls. Neither affected the degree or duration of muscle paralysis (Fig. 2B). In contrast, injecting as little as 60 ng of A8-^{ci}BoNT/XA reduced muscle paralysis (Fig. 2B). Injecting 600 ng of A8-^{ci}BoNT/XA restored muscle function (reaching a score of 0) within 3 days, and increasing the dose to 6 μg yielded similar results (Fig. 2B). The effect is specific for BoNT/A, because A8-^{ci}BoNT/XA did not alter the degree and duration of paralysis induced by BoNT/B (fig. S6, A and B). Furthermore, A8-^{ci}BoNT/XC and A8-^{ci}BoNT/XD reduced BoNT/A-induced leg muscle paralysis as well, albeit requiring higher doses than A8-^{ci}BoNT/XA (fig. S6, C and D). Because A8-^{ci}BoNT/XA is the most effective one in vivo, we focused on A8-^{ci}BoNT/XA hereafter.

To further confirm that A8-^{ci}BoNT/XA shortens muscle paralysis after toxin entry into motor neurons, we waited to inject A8-^{ci}BoNT/XA until day 3 or 6 after the initial BoNT/A injection, by which time paralysis is already decreasing (Fig. 2C, day 3 in red and day 6 in blue). Injecting 600 ng of A8-^{ci}BoNT/XA to the same site where BoNT/A was injected restored muscle function within 1 day for both 3 and 6 days after injection of BoNT/A (Fig. 2C). More frequent monitoring of the degree of muscle paralysis revealed that the DAS score showed an obvious decrease 6 hours after injection of A8-^{ci}BoNT/XA and that muscle function was completely recovered by 15 hours (Fig. 2D). Recovery of a similar speed was achieved with 60 ng of A8-^{ci}BoNT/XA (Fig. 2D), whereas the control mixture of separated A8 and ^{ci}BoNT/XA proteins showed no effect on the degree or duration of muscle paralysis (fig. S6E).

Intraperitoneal injection of A8-^{ci}BoNT/XA shortens BoNT/A-induced leg muscle paralysis

We next analyzed whether A8-^{ci}BoNT/XA can effectively reach the paralyzed leg muscle through systemic circulation. We first injected BoNT/A (6 pg) to the hind leg muscle and waited 18 hours for the muscle to be paralyzed. A8-^{ci}BoNT/XA was then injected intraperitoneally, and the DAS scores were monitored (Fig. 2E). Injecting A8-^{ci}BoNT/XA reduced the local leg muscle paralysis and DAS scores, although a much higher dose of A8-^{ci}BoNT/XA is required compared with the previous intramuscular injection of A8-^{ci}BoNT/XA to the same BoNT/A injection site. The effective dose can be lowered with multiple administrations of A8-^{ci}BoNT/XA. For instance, intraperitoneal injection of 6 μg of A8-^{ci}BoNT/XA daily for 2 days elicited a recovery rate similar to a single dose of 600 μg, whereas dosing with 6 μg daily for 7 days achieved an even faster recovery rate (Fig. 2F). As controls, injecting a total of 600 μg separated A8 and ^{ci}BoNT/XA, or 7 days of daily injections of A8 and ^{ci}BoNT/XA, did not affect the degree or duration of muscle paralysis (fig. S6, F and G).

Intraperitoneal injection of A8-^{ci}BoNT/XA rescues mice from systemic BoNT/A intoxication

We then examined whether A8-^{ci}BoNT/XA can treat systemic BoNT/A intoxication. Intraperitoneal injection of a lethal dose (19.5 pg) of BoNT/A induced systemic botulism symptoms of a "wasp" body shape and reduced mobility in 9 hours in mice, and all mice further developed immobility and severe respiratory stress that required euthanization within a few more hours. To quantify the disease progress, we developed a scoring system based on the

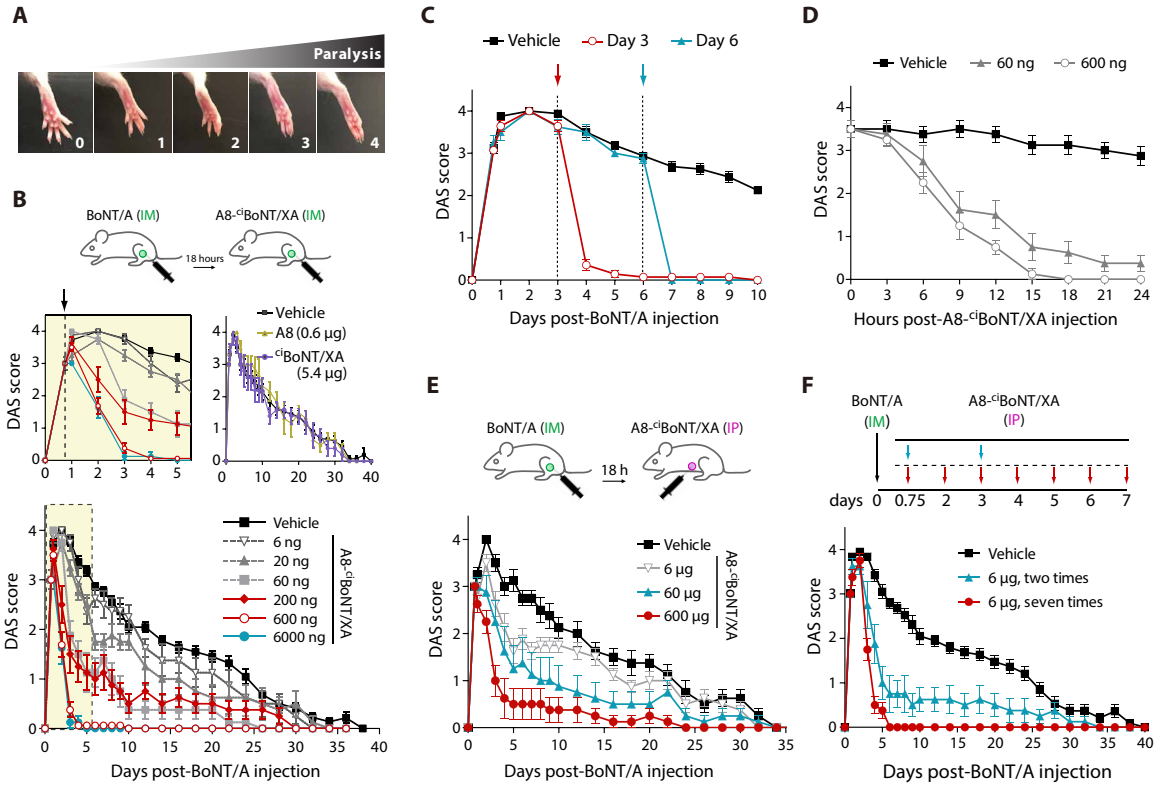

Fig. 2. Post-exposure treatment of BoNT/A-induced local paralysis using A8-^{ci}BoNT/XA. (**A**) Schematic illustration of the DAS assay and representative images showing the degrees of toe spreading. Score "0" represents no paralysis, and score "4" represents the most severe paralysis. (**B**) The indicated amounts of A8-^{ci}BoNT/XA were injected into the mouse hind leg muscle 18 hours after the initial injection of BoNT/A (6 pg). DAS scores were recorded and plotted over time. The DAS scores in the first 5 days were enlarged (top left, an arrow indicates the time of injecting A8-^{ci}BoNT/XA). Injection of A8 or ^{ci}BoNT/XA alone served as controls (top right). Vehicle, $n = 22$; A8-^{ci}BoNT/XA at 6000, 200, 60, and 20 ng, $n = 8$; A8-^{ci}BoNT/XA at 600 ng, $n = 16$. IM, intramuscular injection. (**C**) A8-^{ci}BoNT/XA (600 ng) were injected intramuscularly into the leg muscle 3 days (red) or 6 days (blue) after the initial injection of BoNT/A (6 pg) to the same muscle, and the DAS scores were plotted over time (vehicle, $n = 16$; A8-^{ci}BoNT/XA at day 3, $n = 14$; A8-^{ci}BoNT/XA at day 6, $n = 8$). (**D**) A8-^{ci}BoNT/XA (600 and 60 ng) were injected into the leg muscle 3 days after the initial injection of BoNT/A (6 pg). DAS scores were recorded every 3 hours for 24 hours ($n = 8$ per group). (**E**) A8-^{ci}BoNT/XA at the indicated doses was administered via intraperitoneal injection (IP) 18 hours after the initial injection of BoNT/A (6 pg) to the leg muscle. DAS scores were plotted over time ($n = 8$ per group). (**F**) A8-^{ci}BoNT/XA (6 μg per mouse, IP) was injected either twice (blue, 18 and 42 hours) after the initial injection of BoNT/A (6 pg, IM) to the leg muscle or once per day for 7 days (red, with the first one 18 hours after the initial injection of BoNT/A). Vehicle, $n = 19$; A8-^{ci}BoNT/XA, $n = 8$. (B to F) Data were analyzed by two-way ANOVA with Sidak's post hoc tests, and results and *P* values are shown in table S4.

appearance of the wasp shape, the degree of mobility/activity, respiratory distress, and body weight changes (table S2). Mice were first injected with BoNT/A (19.5 pg, intraperitoneally), and intraperitoneal injection of A8-^{ci}BoNT/XA was then carried out 9 hours later in animals that developed botulism symptoms (Fig. 3A). Injecting 0.6 μg of A8-^{ci}BoNT/XA per mouse reduced the rate of increase in the clinical score, but these mice eventually developed severe symptoms and lost ~20% body weight within 48 hours; all were euthanized (Fig. 3, B to D). A8-^{ci}BoNT/XA at 6 μg per mouse reduced clinical scores within 8 hours, but 1 mouse (of 10) relapsed by 36 hours and was euthanized. Further increasing A8-^{ci}BoNT/XA to 30 μg per mouse reduced clinical score and restored mobility/activity within 6 hours. Body weight gains were comparable with those in control mice and no mice relapsed, suggesting full and complete recovery (Fig. 3, B to D, and movie S1). As controls, mixtures of A8 and ^{ci}BoNT/XA proteins did not offer any protection in this post-exposure model (Fig. 3, B and C, and movie S1).

Two tandemly fused nanobodies can be delivered into neurons

We then evaluated whether multiple nanobodies can be delivered simultaneously by ^{ci}BoNT/XA. We selected a nanobody raised against LC/B in alpaca (known as VHH-BLc-JNE-B10, here abbreviated J10) (*51*). A8 and J10 were fused in tandem to the N terminus of ^{ci}BoNT/XA, and the fusion protein was expressed and purified in *E. coli* (termed A8-J10-^{ci}BoNT/XA; Fig. 4A and fig. S7A). A8-J10-^{ci}BoNT/XA can be activated by thrombin and separated into two fragments, A8-J10-^{ci}LC/X and H_N-H_C, in the presence of DTT (fig. S7A). A8-J10-^{ci}BoNT/XA was able to reduce both cleavage of VAMP2 by LC/B and cleavage of SNAP-25 by LC/A in the rat brain lysates in vitro (fig. S7, B and C).

We next compared the translocation efficacy of two fused nanobodies (A8-J10) versus a single nanobody (A8). A construct expressing A8-J10 fused with the active form of LCH_N/X was generated (A8-J10-LCH_N/X). A8-J10-LC/X cleaved VAMP2 with efficacy similar to A8-LC/X in vitro, indicating that fusion with A8-J10 does not affect the activity of LC/X (fig. S7D). A8-J10-LCH_N/X was then ligated with H_C/A using sortase to generate the active form A8-J10-BoNT/XA (fig. S7E). Translocation efficacy was compared by examining cleavage of VAMP2 in cultured neurons exposed to ligated active toxins. Exposure to picomolar A8-J10-BoNT/XA resulted in cleavage of VAMP2, and the degree of cleavage was similar to that

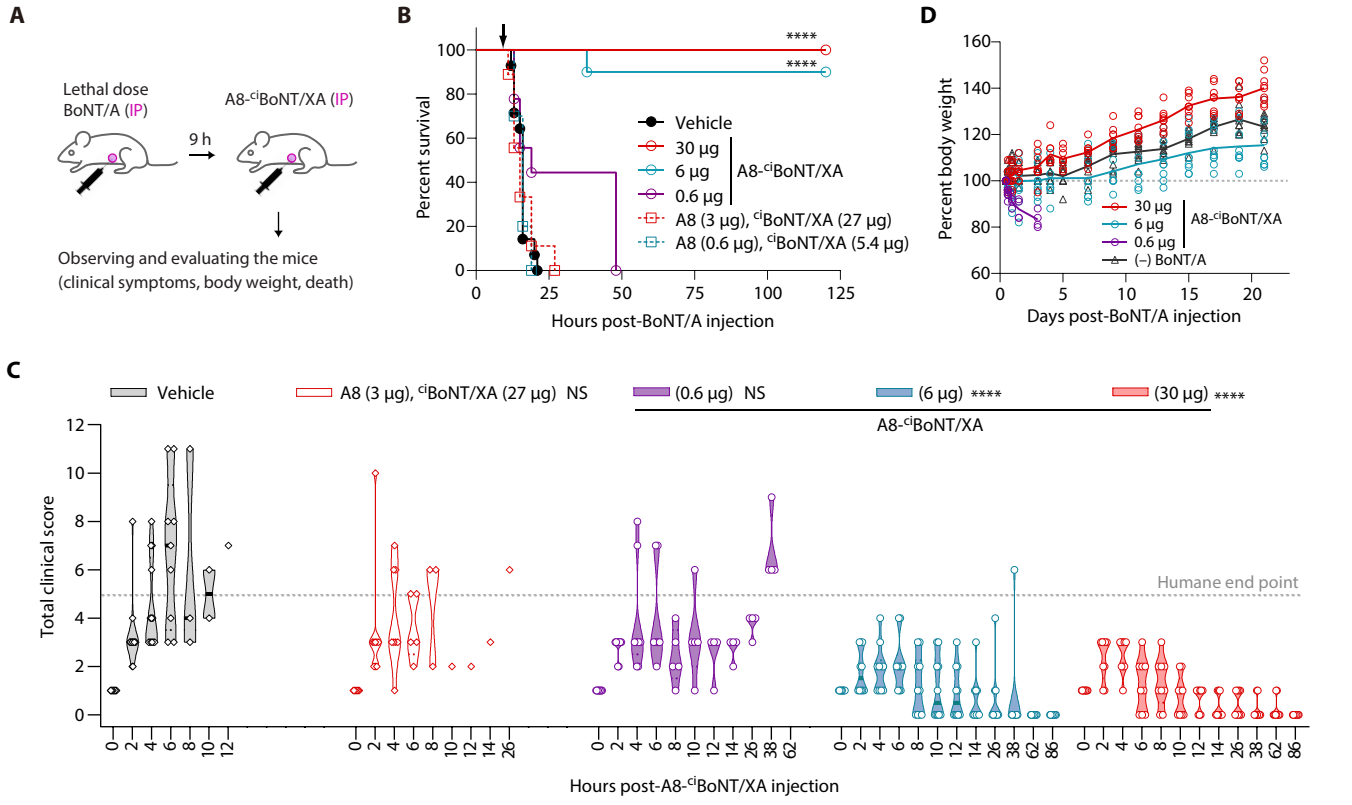

Fig. 3. Post-exposure treatment of systemic toxicity of BoNT/A using A8-^{ci}BoNT/XA. (**A**) Systemic toxicity model of botulism and post-exposure treatment using A8-^{ci}BoNT/XA. Lethal dose of BoNT/A (19.5 pg) was first injected into mice intraperitoneally to induce systemic botulism. A8-^{ci}BoNT/XA or the control mixture of A8 and ^{ci}BoNT/XA proteins were injected intraperitoneally 9 hours later when botulism symptoms had developed. (**B** to **D**) Experiments were carried out as described in (A) with the indicated concentrations of A8-^{ci}BoNT/XA and the control A8/^{ci}BoNT/XA mixture [vehicle, n = 14; A8-^{ci}BoNT/XA at 30 and 0.6 μg, n = 9; A8-^{ci}BoNT/XA at 6 μg, n = 10; A8 (3 μg)/^{ci}BoNT/XA (27 μg), n = 9; A8 (0.6 μg)/^{ci}BoNT/XA (5.4 μg), n = 10]. Survival rates are plotted in (B) (statistical analysis was conducted by log-rank test; ****P < 0.0001). Violin plots of clinical scores of each mouse are shown in (C). The humane end point was set as clinical scores above 5. Data were analyzed by nested one-way ANOVA with Dunnett's post hoc tests, ****P < 0.0001. NS, not significant. Statistical analysis results and P values for (D) are shown in table S4.

of neurons exposed to the same concentrations of A8-BoNT/XA (fig. S7F), suggesting that LC/X fused with two nanobodies was delivered into the cytosol of neurons as efficiently as the one fused with a single nanobody.

We further assessed the ability of A8-J10-^{ci}BoNT/XA to inhibit LC/A within neurons. Neurons were exposed to BoNT/A for 12 hours, washed, incubated for another 24 hours, and then incubated with A8-J10-^{ci}BoNT/XA for 48 hours. A8-^{ci}BoNT/XA and a mixture of separated A8-J10 and ^{ci}BoNT/XA were analyzed in parallel as controls. Cell lysates were analyzed by immunoblot, detecting cleavage of SNAP-25 by LC/A. Incubation with A8-J10-^{ci}BoNT/XA reduced cleavage of SNAP-25, whereas the control mixture of A8-J10 and ^{ci}BoNT/XA did not affect cleavage of SNAP-25 (fig. S7G). Incubation with A8-^{ci}BoNT/XA resulted in a larger reduction in cleavage of SNAP-25 compared with the same concentrations of A8-J10-^{ci}BoNT/XA (fig. S7G), suggesting that A8-J10-^{ci}BoNT/XA showed lower efficacy in inhibiting LC/A in the cytosol of neurons compared with A8-^{ci}BoNT/XA.

A8-J10-^{ci}BoNT/XA can treat both BoNT/A and BoNT/B intoxication in vivo

We then tested A8-J10-^{ci}BoNT/XA in vivo in mice. Like A8-^{ci}BoNT/XA, A8-J10-^{ci}BoNT/XA showed no toxicity after intraperitoneal injection at 100 mg/kg (table S1). We first carried out DAS assays with injection of BoNT/A (Fig. 4B) or BoNT/B (BoNT/B-induced paralysis lasts ~10 to 12 days in mice; Fig. 4C) to the hind leg. Intramuscular injection of A8-J10-^{ci}BoNT/XA to the same site 18 hours later reduced DAS scores and shortened the duration of paralysis in a concentration-dependent manner for BoNT/A and BoNT/B. Muscle function was completely restored within 3 days for BoNT/A and within 2 days for BoNT/B after injection of A8-J10-^{ci}BoNT/XA, whereas the control mixture of A8-J10 and ^{ci}BoNT/XA did not affect the degree or duration of paralysis (Fig. 4, B and C). A8-J10-^{ci}BoNT/XA appeared to be less potent than A8-^{ci}BoNT/XA, because 6.5 μg is required to reduce DAS score to a similar degree as 600 ng of A8-^{ci}BoNT/XA (Figs. 2B and 4B). Further optimization of the A8-J10-^{ci}BoNT/XA protein might be needed to enhance its efficacy.

We finally examined the capability of A8-J10-^{ci}BoNT/XA to rescue mice from systemic toxicity of BoNT/A and BoNT/B, using the post-exposure intraperitoneal injection model described in Fig. 3. Intraperitoneal administration of A8-J10-^{ci}BoNT/XA at 32.5 μg per mouse, 9 hours after preinjection of lethal doses of BoNT/A, rescued mice from death (Fig. 4D), reduced clinical scores (Fig. 4E and movie S2), and eliminated body weight reduction (Fig. 4F). Lower concentrations (6.5 μg per mouse) elicited partial effects, whereas the control mixture of A8-J10 and ^{ci}BoNT/XA showed no effect (Fig. 4, D to E, and movie S2). Similar experiments were carried out with a lethal dose of BoNT/B (10 pg). Injection of A8-J10-^{ci}BoNT/XA

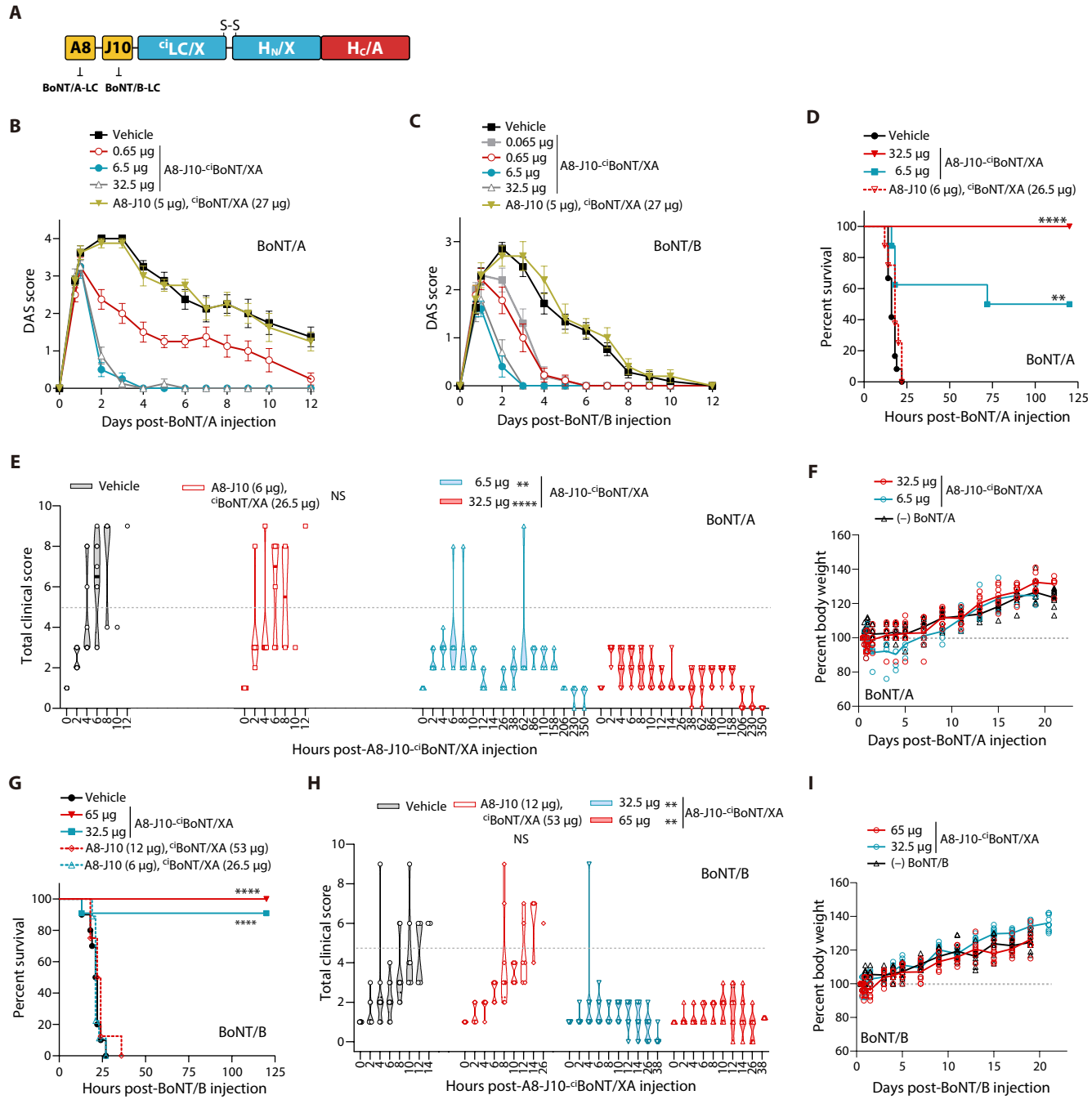

Fig. 4. Delivery of two nanobodies using ciBoNT/XA for post-exposure treatment of BoNT/A and BoNT/B intoxication. (**A**) Schematic drawing of ciBoNT/XA with two nanobodies (A8 against LC/A and J10 against LC/B) fused to its N terminus. The fusion protein is termed A8-J10-ciBoNT/XA. (**B** and **C**) DAS assays were carried out with BoNT/A [6 pg, (B)] or BoNT/B [3.5 pg, (C)]. The indicated concentrations of A8-J10-ciBoNT/XA were injected into the same leg muscle 18 hours later, and DAS scores were plotted over time [(B) vehicle, $n = 9$; A8-J10-ciBoNT/XA of each group and A8-J10 (5 μg)/ciBoNT/XA (27 μg), $n = 8$; (C) vehicle, $n = 27$; A8-J10-ciBoNT/XA at 30, 6, and 0.06 μg, $n = 10$; at 0.6 μg, $n = 9$]. Data were analyzed by two-way ANOVA with Dunnett's post hoc tests, and results and P values are shown in table S4. (**D** to **F**) Lethal doses of BoNT/A (19.5 pg) were injected via intraperitoneal administration into mice to induce systemic botulism. The indicated concentrations of A8-J10-ciBoNT/XA were injected intraperitoneally 9 hours after injection of BoNT/A. Mixtures of A8-J10 and ciBoNT/XA served as controls. Survival rates (D), clinical scores (E), and body weight changes (F) are shown (vehicle, $n = 12$; other groups, $n = 8$). ****$P < 0.0001$ and **$P = 0.00022$ (log-rank test). Statistical analysis results and P values for (F) are shown in table S4. (**G** to **I**) Lethal doses of BoNT/B (10 pg) were injected via intraperitoneal administration into mice to induce systemic botulism. The indicated concentrations of A8-J10-ciBoNT/XA were injected intraperitoneally 9 hours after injection of BoNT/B. Survival rates (G), clinical scores (H), and body weight changes (I) are shown [vehicle, $n = 10$; A8-J10-ciBoNT/XA at 65 μg, $n = 8$; at 32.5 μg, $n = 11$; A8-J10 (12 μg)/ciBoNT/XA (53 μg), $n = 8$; A8-J10 (6 μg)/ciBoNT/XA (26.5 μg), $n = 9$]. ****$P < 0.0001$ (log-rank test). Data were analyzed by log-rank test (D and G) or nested one-way ANOVA with Dunnett's post hoc tests (E and H), **$P < 0.01$ and ****$P < 0.0001$. Statistical analysis results and P values for (I) are shown in table S4.

showed concentration-dependent rescue from death (Fig. 4G), reduction in botulism symptoms (Fig. 4H and movie S3), and elimination of body weight reduction (Fig. 4I), with complete rescue achieved at 65 μg per mouse, whereas the control mixture of A8-J10 and ^{ci}BoNT/XA showed no effect (Fig. 4, G to H, and movie S3).

DISCUSSION

Development of biological drugs (biologics) such as proteins and antibodies has revolutionized many therapeutic areas. However, current biologics are largely limited to acting on cell surface targets. Intracellular proteins and processes represent vast untapped drug targets, yet the cell membrane forms a formidable barrier. In addition, the ability to target a cell type specifically is another major challenge for drug delivery to enhance therapeutic efficacy and minimize side effects. Here, we developed a protein-based drug delivery platform that achieves both highly specific targeting of neurons and successful delivery of therapeutics into the cytosol of cells.

The effectiveness of this platform has been fully validated using BoNT intoxication models in vivo in mice. An anti-BoNT/A therapeutic protein was created by fusing a nanobody (A8) against LC/A to the N terminus of the delivery protein. Using cultured neurons, we demonstrate that A8 was delivered into the cytosol of neurons in vitro and neutralized LC/A. Intramuscular injection of this therapeutic protein 3 or 6 days after the initial injection of BoNT/A restored muscle activity within 15 hours in a local leg muscle paralysis model in mice. Intraperitoneal administration of this therapeutic protein rescued mice from systemic toxicity of BoNT/A after botulism symptoms developed.

The delivery platform is a 150-kDa chimeric protein, with one-third derived from the H_C of a BoNT and two-thirds derived from the recently discovered BoNT-like toxin BoNT/X. The H_C of BoNT confers specificity toward neurons. The BoNT/X fragment includes a catalytically inactive form of LCH_N. The key finding here is that the chimeric protein containing $^{ci}LCH_N$/X showed no toxicity in mice even at 100 mg/kg, which allowed us to create a safe and effective protein-based delivery platform.

The molecular basis for the lack of toxicity of $^{ci}LCH_N$/X in mice remains to be determined. BoNT/X is a recently identified BoNT-like toxin, sharing ~28 to 30% sequence identity with other BoNTs and the overall conserved domain arrangement (*42*). Besides BoNT/X, two other BoNT-like toxins have been recently reported: one is BoNT/En, identified in an *Enterococcus faecium* strain (*52*, *53*), which shares 24 to 27% protein sequence identity to other BoNTs and 37% identity to BoNT/X. BoNT/En showed no toxicity in mice, and replacing its H_C with H_C/A resulted in a chimeric toxin that potently induced muscle paralysis in mice, suggesting that mice lack the proper receptor for BoNT/En. The other BoNT-like toxin is designated paraclostridial mosquitocidal protein 1 (PMP1), identified by screening bacteria that kill *Anopheles* mosquito larvae (*54*). PMP1 shares 36% protein sequence identity with BoNT/X and 34% with BoNT/En. The natural hosts targeted by BoNT/X and BoNT/En remain unknown, whereas PMP1 appears to target mosquito larvae. It will be interesting to characterize $^{ci}LCH_N$ of BoNT/En and PMP1 to determine whether they share the same properties of no toxicity in mice as $^{ci}LCH_N$/X.

We constructed and tested fusion of $^{ci}LCH_N$/X to three different H_Cs: H_C/A, H_C/C, or H_C/D. A8-^{ci}BoNT/XA and A8-^{ci}BoNT/XC showed similar efficacy in reducing SNAP-25 cleavage in cultured neurons, but 60 ng of A8-^{ci}BoNT/XA achieved better reduction in paralysis in DAS assays than 6 μg of A8-^{ci}BoNT/XC in vivo. These data suggest that A8-^{ci}BoNT/XC is less effective (or less stable) in vivo compared with A8-^{ci}BoNT/XA. A8-^{ci}BoNT/XD showed lower efficacy in reducing SNAP-25 cleavage than A8-^{ci}BoNT/XA and A8-^{ci}BoNT/XC, and its in vivo efficacy is lower than A8-^{ci}BoNT/XC. These data indicate that the choice of H_C affects delivery and in vivo efficacy. Potential structural conflicts between $^{ci}LCH_N$ and H_C might contribute to instability of the protein in vivo. It will be interesting to further optimize the choice of H_Cs, because an alternative H_C other than H_C/A has the benefit of not immunizing patients against BoNT/A, thus preserving the possibility of treating patients with BoNT/A in the future.

As expected, A8-^{ci}BoNT/XA shares the BoNT/A receptor, SV2, which is a family of synaptic vesicle membrane proteins including SV2A, SV2B, and SV2C. The exposure of SV2 to the cell surface is reduced after synaptic vesicle exocytosis is blocked by BoNTs. However, SV2 still travels to cell surfaces during its nascent biogenesis before it is internalized and sorted onto synaptic vesicles, and this constitutive secretory pathway is not affected by any BoNTs (*55*, *56*), which likely provides an entry pathway for A8-^{ci}BoNT/XA after synaptic vesicle exocytosis is blocked by preloaded BoNT/A.

Our studies suggest that two tandemly fused nanobodies can be translocated into the cytosol of neurons as efficiently as a single nanobody. This allows us to develop a single agent that can target two distinct toxins. Furthermore, dimers of two nanobodies targeting the same toxin may also be used to enhance the binding and inhibition of the target toxin as previously reported (*57*). It will be interesting to explore how many more nanobodies can be delivered without reducing membrane translocation efficacy.

Nanobodies are one of the most versatile small antibody–derived protein binders that can be readily developed against proteins of interest. Besides binding and inhibiting the target protein directly, the therapeutic potential of nanobodies might be further enhanced by promoting degradation of the target protein via fusion with a protein degradation signal (degron) or a moiety that recruits E3-ubiquitin ligase. This is similar to the proteolysis-targeting chimeras (PROTACs) approach (*58*, *59*), but using nanobodies rather than chemical probes for targeting the protein of interest. It has been shown that expression of A8 fused with a 15-kDa F-box domain, which recruits E3-ubiquitin ligase, accelerated degradation of LC/A in cells (*43*). More generally, the approach of fusing of a nanobody to a protein domain recruiting E3-ubiquitin ligase to induce degradation of the target protein has been well established in cells and in model organisms (*60*–*64*). However, these previous studies lacked a way to deliver the fusion protein into cells and relied on transfection or transgenic approaches. The delivery platform reported here might enable the use of nanobody fusion proteins or nanobody conjugated with a chemical ligand to induce degradation of intracellular targets. In addition, delivery of nanobodies can be achieved using platforms based on other bacterial toxins such as heat-labile enterotoxin IIa, which has been shown to deliver A8 into the cytosol of cultured neurons (*65*).

The range of proteins that can be efficiently delivered by our delivery platform remains to be explored experimentally. Bade *et al.* (*30*) showed that the translocation efficacy of proteins fused to BoNT/D is influenced not only by size but also, more importantly, by structural rigidity. For instance, firefly luciferase (62 kDa) fused to BoNT/D was translocated into neurons at a higher rate than GFP (27 kDa). Furthermore, fusion of DHFR (25 kDa) to BoNT/D did

not affect translocation of BoNT/D, but when DHFR is stabilized by binding to the folate analog Mtx, it reduced translocation of the fusion protein by 10-fold.

Because of technical limitations, experimental evidence directly detecting binding of our therapeutic fusion proteins to motor nerve terminals and cytosolic delivery of nanobodies in vivo remain to be established. In addition, pharmacokinetic and pharmacodynamic studies and evaluation of long-term safety of these fusion proteins also need to be carried out. Our current study is limited to mouse models, and it will be crucial to extend the study to additional animal models.

The major limiting factor for any protein-based delivery platform is likely the generation of neutralizing antibodies over time, which renders repeated usage less effective. This issue could be ameliorated through additional protein engineering of deimmunization. This, however, should not be an issue for treating botulism, which likely involves only a single treatment event.

In summary, we created a neuron-specific delivery platform based on a chimeric toxin approach by combining the neuronal specificity of BoNT-H_C and the unique nontoxic property of the deactivated LCH_N of BoNT/X. On the basis of this platform, we developed a safe and effective post-exposure treatment for BoNT/A and BoNT/B. The modular nature of our chimeric toxins offers a general approach to targeting distinct cell types by changing the receptor-binding domain. Furthermore, different types of cargoes, such as therapeutic peptide/proteins, small molecules, and DNA/RNA, can be conjugated to the delivery system, with the potential to modulate previously hard-to-reach cytosolic targets.

METHODS

Study design

The objective of this study is to establish a drug delivery platform to target and inhibit BoNTs within the cytosol of neurons. We created a chimeric toxin–based delivery vehicle and used nanobodies against BoNTs as therapeutic cargoes. The nanobody-delivery vehicle fusion proteins were expressed in *E. coli* and purified as His6-tagged proteins. We first evaluated their toxicity to mice via intraperitoneal injections and then examined the delivery of nanobodies into the cytosol of cultured rat cortical neurons, followed by assessing the therapeutic effect in vivo using both a local muscle paralysis model and a systemic toxicity model in mice. The sample sizes were selected on the basis of previous literature and noted in each figure legend. The humane end point was defined on the basis of clinical scores and body weight reduction (table S2). Mice were randomly assigned to either treatment or control groups. The number of replications was noted in each figure legend. For all animal experiments, investigators were not blinded to the treatment/control groups or the data analysis. All procedures using mice were conducted in accordance with the guidelines approved by the Institute Animal Care and Use Committee at Boston Children's Hospital (#18-10-3794R). The Institutional Review Entity at Boston Children's Hospital has reviewed and determined that the work does not fall under Dual Use Research of Concern.

Materials

Goat Anti-llama IgG H&L (HRP) (ab112786, 1:500) was purchased from Abcam (Cambridge). Mouse monoclonal antibodies for syntaxin 1 (Cl 78.2, 1:3000), SNAP-25 (Cl 71.1, 1:2000), and VAMP2 (Cl 69.1, 1:1000) were purchased from Synaptic Systems (Göttingen, Germany). The following antibodies were purchased from the indicated vendors: rabbit polyclonal antibody for synapsin (Millipore) and mouse monoclonal antibody for actin (AC-15, 1:1000; Sigma-Aldrich). The human monoclonal antibody against BoNT/A (Raz-1, 1:1000) was provided by J. Lou and J. Marks (San Francisco, CA). BoNT/A and BoNT/B were purchased from Metabiologics (Madison, WI, USA).

Plasmid construction

The complementary DNAs (cDNAs) encoding A8 (GenBank: FJ643070.1) and J10 were synthesized by Integrated DNA Technologies (Coralville, Iowa) (*51*). The composition of all constructs in this study is summarized in table S3. The cDNAs encoding ^{ci}BoNT/XA (LC/X, residues 1 to 422; H_N/X, residues 468 to 924; H_C/A, residues 873 to 1296) were cloned into pET28a vector with a His6 tag fused to its C terminus. Three amino acids in LC/X were mutated (residues E228Q, R360A, and Y363F) by site-directed mutagenesis. Three thrombin cleavage sites were introduced to the locations between LC/X and H_N/X, between H_C and the His6 tag, and between the N-terminal thioredoxin tag (TrxA) and LC/X. A8-^{ci}BoNT/XA, A8-^{ci}BoNT/XC, and A8-^{ci}BoNT/XD chimera (H_C/C, residues 868 to 1291; H_C/D, residues 864 to 1276) were cloned into pET28a vectors with His6 tag on their C termini. Flexible 10–amino acid linker $(Gly4Ser)_2$ was introduced between A8 and LC/X. ^{ci}BoNT/C (E230Q, R372A, and Y375F), A8-^{ci}BoNT/C, and ^{ci}BoNT/A (E224Q, R363A, and Y366F) were subcloned into pET28a vector. A8, J10, and A8-J10 were cloned into pET28a vector with TrxA tag at N termini and His6 tag at C termini. A8-J10-^{ci}BoNT/XA was cloned into pET28a vector. LCH_N/X, A8-LCH_N/X, and A8-J10-LCH_N/X were cloned into pET28a vector with the sortase tag sequence "LPETGG" fused to their C termini, followed by a His6 tag. Rat SV2C-L4 (residues 473 to 567) and rat VAMP2 (residues 1 to 93) were cloned into pGEX-4T-1. The construct encoding His6-tagged sortase (SrtA*) was provided by B. Pentelute (Boston, MA, USA).

Protein expression, purification, and activation

Plasmids were transformed into *E. coli* BL21 (DE3). Cells were cultured at 37°C and 300 rpm shaking in 2-liter baffled flasks containing 400 ml of autoinduction medium (Formedium). Once the OD_{600} (optical density at 600 nm) reached 0.4 to 0.6, the temperature was decreased to 16°C and further incubated for 18 to 24 hours. The cells were harvested at 4000 rpm for 30 min and stored at −80°C. For A8-J10-^{ci}BoNT/XA expression, the plasmid was transformed into SHuffle T7 Express *E. coli* (New England Biolabs, Beverly, MA). Cells were cultured at 30°C and 250 rpm shaking in 2-liter baffled flasks containing 1000 ml of Terrific Broth medium. Expression was induced with 0.4 mM isopropyl-β-D-thiogalactopyranoside (IPTG) when OD_{600} reached 0.5 to 0.8, then the temperature was decreased to 16°C, and further cultured for 18 hours. The cells were harvested at 4000 rpm for 30 min and stored at −80°C.

Bacteria were disrupted by sonication in the binding buffer [20 mM tris-HCl (pH 7.5), 500 mM NaCl, 10% glycerol, 20 mM imidazole, 1 mM phenylmethylsulfonyl fluoride]. Lysates were centrifuged at 20,000 rpm for 30 min at 4°C. The supernatant was loaded onto a HisTrap HP (5 ml; GE Healthcare) and washed with the binding buffer. Proteins were eluted by a linear gradient of 20 to 250 mM imidazole over 50 ml. Target proteins were collected on the basis of molecular weight and concentrated using Vivaspin

[100-kDa molecular weight cutoff (MWCO); GE Healthcare]. To generate the di-chain form of ^{ci}BoNT, proteins were proteolytically cleaved with thrombin (2 U/mg protein; Millipore) at 4°C overnight. The proteins were further purified using size exclusion column (Superdex 200 pg 16/60, GE Healthcare) in 20 mM tris-HCl (pH 7.5) and 150 mM NaCl. The elution peak was collected and concentrated using Vivaspin (100-kDa MWCO). Proteins were filtered through an endotoxin removal resin (Thermo Fisher Scientific) and sterilized using 0.22-μm filters (Millipore). Purified proteins were aliquoted (50 to 100 μl per tube) and stored at −80°C.

A8 and A8-J10 were purified using HisTrap columns. For removing the TrxA tag, the elution was treated with thrombin at 4°C overnight and passed through a PD-10 column (GE Healthcare) equilibrated with the binding buffer. Elutions were incubated with Ni-NTA beads at room temperature (RT) for 30 min and washed three times using the binding buffer. A8 and A8-J10 were eluted using 250 mM imidazole and concentrated using Vivaspin (10-kDa MWCO). The proteins were further purified using size exclusion column (Superdex 75 10/30, GE Healthcare) in 20 mM tris-HCl (pH 7.5) and 150 mM NaCl. LCH_N/X, A8-LCH_N/X, A8-J10-LCH_N/X, and H_C/A were purified using HisTrap and size exclusion (Superdex 200 pg 16/60) columns in 20 mM tris-HCl (pH 7.5), 150 mM NaCl, and 10% glycerol.

Neuron cultures

Pregnant rats were purchased from Charles River. Twenty-four–well plates were coated with poly-D-lysine (0.5 mg/ml in deionized water) at 37°C for 3 hours and washed three times with deionized water. Primary rat cortical neurons were prepared from embryonic day 18 (E18) and E19 embryos using a papain dissociation kit (Worthington Biochemical). Pregnant rats were euthanized by CO_2 asphyxiation, and embryos were removed. Dissected cortical tissue was dissociated in papain solution at 37°C for 60 min. Cortical neurons were plated on poly-D-lysine–coated 24-well plates at a density of 250,000 cells per well (for Western blot) or 150,000 cells per well (for immunostaining) in 1 ml of culture medium (Neurobasal medium plus B27 and 0.5% fetal bovine serum).

Detection of nanobody in the cytosol of neuron

Neurons were exposed to A8-^{ci}BoNT/XA with or without 100 nM bafilomycin A1 (B1793; Sigma-Aldrich) in medium for 12 hours. Cells were washed with phosphate-buffered saline (PBS) three times and lysed with 100 μl of lysis buffer [PBS containing 1% Triton X-100, 0.05% SDS, and protease inhibitor cocktail tablet (Thermo Fisher Scientific)]. Lysates were centrifuged for 10 min at 4°C. The supernatant was mixed with SDS sample buffer [62.5 mM tris-HCl (pH 6.8), 2% SDS, 10% glycerol, and 0.005% bromophenol blue] without DTT and subjected to immunoblot analysis under nonreducing conditions to detect translocated A8-^{ci}LC/X. A8-^{ci}LC/X and A8-^{ci}BoNT/XA were detected using horseradish peroxidase (HRP)–conjugated goat anti-llama immunoglobulin G (IgG) with Clarity Max Western ECL Substrate (Bio-Rad, #1705062).

Post-exposure inhibition of BoNT/A in cultured cortical neurons

Neurons were cultured in 1.5-ml cultured medium. After 11 days in vitro, 1200 μl of culture medium was collected and used as a conditioned medium. Neurons were exposed to 20 pM BoNT/A in 300-μl medium at 37°C for 12 hours. Cells were washed two times with the medium to remove residual BoNTs and incubated in 300 μl of the conditioned medium for 24 hours. Neurons were further exposed to A8-^{ci}BoNT/XA in 400-μl medium for 48 hours and then lysed with 200-μl lysis buffer. Lysates were centrifuged for 10 min at 4°C. Supernatants were subjected to SDS–polyacrylamide gel electrophoresis (PAGE) and immunoblot analysis.

Immunostaining

A8-^{ci}BoNT/XA (200 nM) and glutathione *S*-transferase (GST)–SV2C-L4 (2 μM) were incubated for 20 min at 37°C. Neurons were exposed to the mixture in medium for 8 min at 37°C. Cells were washed with ice-cold PBS and fixed with PBS containing 4% paraformaldehyde for 20 min at RT. Cells were treated with blocking buffer (PBS containing 10% goat normal serum) for 45 min and exposed to human anti-BoNT/A antibody (1:500) and rabbit anti-synapsin antibody (1:600) in blocking buffer at 4°C overnight. Cells were washed with PBS and incubated with Alexa Fluor 488 goat anti-human IgG and Alexa Fluor 546 goat anti-rabbit IgG (1:800) in blocking buffer for 1 hour. The coverslip was then mounted on a slide, and images were collected using a fluorescence microscope (Olympus IX81).

Sortase-mediated ligation and assessing translocation efficacy

His6-tagged H_C/A was cleaved overnight at 4°C by thrombin to expose the glycine residue at the N terminus. The ligation reaction was set up in 50-μl tris buffer (pH 7.5), with H_C/A (40 μM), LCH_N/X, A8-LCH_N/X, or A8-J10-LCH_N/X (4 μM), Ca^{2+} (10 mM), and sortase (0.5 μM) for 45 min at RT. The ligation products were activated by thrombin treatment (0.4 U) for 30 min at RT. Ligated products were analyzed by SDS-PAGE, and the concentration was quantified using ImageJ. Neurons were exposed to ligated products in 300-μl cultured medium for 12 hours at 37°C. Cell lysates were subjected to immunoblot analysis detecting cleavage of VAMP2.

Cleavage of recombinant VAMP2 by LC/X, A8-LC/X, and A8-J10-LC/X

VAMP2 (residues 1 to 93) was expressed and purified as a GST-tagged protein. LCH_N/X, A8-LCH_N/X, and A8-J10-LCH_N/X were activated with thrombin treatment and incubated with DTT to generate LC/X, A8-LC/X, and A8-J10-LC/X. GST-VAMP2 (4 μM) was incubated with LC/X, A8-LC/X, or A8-J10-LC/X (300, 100, 30, or 10 nM) for 2 min at 37°C. Samples were analyzed by SDS-PAGE and Coomassie blue staining.

Brain detergent extract preparation and in vitro toxin neutralization assay

Rat brain detergent extracts (BDEs) were prepared as previously described (*42*). LC/A (1 μM, final concentration) or LC/B (1 μM) was preincubated with A8, A8-^{ci}BoNT/XA, or A8-J10-^{ci}BoNT/XA in 15 μl of tris buffer (pH 7.5) for 30 min at RT. The mixtures were then added to 15 μl of BDE (2 mg/ml) and incubated for 1 hour at 37°C. Samples were subjected to SDS-PAGE and immunoblot analysis.

DAS assay and post-exposure treatment for local paralysis

Male mice (CD-1 strain, 20 to 30 g) were purchased from Envigo. BoNTs were diluted in 0.2% gelatin-phosphate buffer (pH 6.3). Mice were anesthetized with isoflurane and administered 10 μl of BoNT/A (6 pg) or BoNT/B (3.6 pg) by intramuscular injection into the gastrocnemius muscle of the right hind limb using a 30-gauge needle attached to a Hamilton syringe. The degree of digit abduction was scored on a five-point scale (0, normal; to 4, maximal paralysis; Fig. 2A). These mice were then administered A8-^{ci}BoNT/XA or

A8-J10-^{ci}BoNT/XA in 0.2% gelatin-phosphate buffer (pH 6.3) by intramuscular injection into the same muscle. Mice were monitored once per day for 10 days and then further monitored once every other day until fully recovered from the paralysis.

Mouse lethality assay and systemic post-exposure treatment model

Mice were administered a lethal dose of BoNT/A (19.5 pg) or BoNT/B (10 pg) in 100 μl of 0.2% gelatin-phosphate buffer (pH 6.3) through intraperitoneal injection. After 9 hours, mice that developed typical botulism symptoms such as wasp waist were selected and randomly assigned to either treatment or control groups. These mice were then administered vehicle control (0.2% gelatin-PBS), a mixture of A8 and ^{ci}BoNT/XA, A8-^{ci}BoNT/XA, or A8-J10-^{ci}BoNT/XA in 0.2% gelatin-PBS by intraperitoneal injection. Mice were monitored once per every 2 hours for 14 hours, followed by three times per day for 5 days, and then once every other day for 21 days. Survival rates, clinical scores (table S2), and body weight were recorded. The humane end point was set as total clinical score above 5.

Statistical analysis

Statistical analysis was performed using GraphPad Prism 8.3 software. For all experiments, data are expressed as means ± SEM. The statistical significance of the observed differences was calculated using one- or two-way analysis of variance (ANOVA) (Dunnett's post hoc or Sidak's post hoc tests) or unpaired two-tailed *t* test. Survival curves were analyzed using log-rank (Mantel-Cox) test. Results were considered significant when $P < 0.05$. Statistical analysis data and *P* values for DAS assays and body weight changes (Figs. 2, B to F, 3D, and 4, B, C, F, and I, and fig. S6, B to G) were presented in table S4.

SUPPLEMENTARY MATERIALS

stm.sciencemag.org/cgi/content/full/13/575/eaaz4197/DC1

Fig. S1. Production and characterization of A8-^{ci}BoNT/XA, A8-^{ci}BoNT/XC, A8-^{ci}BoNT/XD, and A8-^{ci}BoNT/C.

Fig. S2. Quantification of A8-^{ci}BoNT/XA translocation in cultured neurons.

Fig. S3. Generating active BoNT/XA and A8-BoNT/XA using sortase-mediated ligation.

Fig. S4. Characterization of A8-^{ci}BoNT/XC and A8-^{ci}BoNT/XD on cultured neuron.

Fig. S5. A8-^{ci}BoNT/XA and ^{ci}BoNT/XA use the same receptors to target neurons as BoNT/A.

Fig. S6. A8-^{ci}BoNT/XA reduces BoNT/A-induced leg muscle paralysis in vivo.

Fig. S7. Characterization of A8-J10-^{ci}BoNT/XA in vitro and on cultured neurons.

Table S1. In vivo toxicity analysis of the indicated proteins.

Table S2. Clinical scores for botulism in mice.

Table S3. Schematic illustration of the indicated constructs.

Table S4. Raw data and statistical analysis (Excel file).

Movie S1. Activity and mobility of mice treated with A8-^{ci}BoNT/XA in a BoNT/A-induced botulism model.

Movie S2. Activity and mobility of mice treated with A8-J10-^{ci}BoNT/XA in a BoNT/A-induced botulism model.

Movie S3. Activity and mobility of mice treated with A8-J10-^{ci}BoNT/XA in a BoNT/B-induced botulism model.

View/request a protocol for this paper from *Bio-protocol*.

REFERENCES AND NOTES

1. M. Dong, G. Masuyer, P. Stenmark, Botulinum and tetanus neurotoxins. *Annu. Rev. Biochem.* **88**, 811–837 (2019).
2. M. Pirazzini, O. Rossetto, R. Eleopra, C. Montecucco, Botulinum Neurotoxins: Biology, pharmacology, and toxicology. *Pharmacol. Rev.* **69**, 200–235 (2017).
3. O. Rossetto, M. Pirazzini, C. Montecucco, Botulinum neurotoxins: Genetic, structural and mechanistic insights. *Nat. Rev. Microbiol.* **12**, 535–549 (2014).
4. M. Montal, Botulinum neurotoxin: A marvel of protein design. *Annu. Rev. Biochem.* **79**, 591–617 (2010).
5. A. Rummel, The long journey of botulinum neurotoxins into the synapse. *Toxicon* **107**, 9–24 (2015).
6. G. Schiavo, M. Matteoli, C. Montecucco, Neurotoxins affecting neuroexocytosis. *Physiol. Rev.* **80**, 717–766 (2000).
7. S. S. Arnon, R. Schechter, T. V. Inglesby, D. A. Henderson, J. G. Bartlett, M. S. Ascher, E. Eitzen, A. D. Fine, J. Hauer, M. Layton, S. Lillibridge, M. T. Osterholm, T. O'Toole, G. Parker, T. M. Perl, P. K. Russell, D. L. Swerdlow, K. Tonat; Working Group on Civilian Biodefense, Botulinum toxin as a biological weapon: Medical and public health management. *JAMA* **285**, 1059–1070 (2001).
8. C. L. Hatheway, in *Clostridial Neurotoxins*, C. Montecucco, Ed. (Springer-Verlag, 1995), vol. 195, pp. 55–75.
9. J. Sobel, Botulism. *Clin. Infect. Dis.* **41**, 1167–1173 (2005).
10. J. E. Keller, E. A. Neale, G. Oyler, M. Adler, Persistence of botulinum neurotoxin action in cultured spinal cord cells. *FEBS Lett.* **456**, 137–142 (1999).
11. R. C. Whitemarsh, W. H. Tepp, E. A. Johnson, S. Pellett, Persistence of botulinum neurotoxin a subtypes 1-5 in primary rat spinal cord cells. *PLOS ONE* **9**, e90252 (2014).
12. Y. C. Tsai, A. Kotiya, E. Kiris, M. Yang, S. Bavari, L. Tessarollo, G. A. Oyler, A. M. Weissman, Deubiquitinating enzyme VCIP135 dictates the duration of botulinum neurotoxin type A intoxication. *Proc. Natl. Acad. Sci. U.S.A.* **114**, E5158–E5166 (2017).
13. S. Pellett, W. H. Tepp, R. C. Whitemarsh, M. Bradshaw, E. A. Johnson, In vivo onset and duration of action varies for botulinum neurotoxin A subtypes 1-5. *Toxicon* **107**, 37–42 (2015).
14. P. G. Foran, N. Mohammed, G. O. Lisk, S. Nagwaney, G. W. Lawrence, E. Johnson, L. Smith, K. R. Aoki, J. O. Dolly, Evaluation of the therapeutic usefulness of botulinum neurotoxin B, C1, E, and F compared with the long lasting type A. Basis for distinct durations of inhibition of exocytosis in central neurons. *J. Biol. Chem.* **278**, 1363–1371 (2003).
15. E. A. Johnson, Clostridial toxins as therapeutic agents: Benefits of nature's most toxic proteins. *Annu. Rev. Microbiol.* **53**, 551–575 (1999).
16. M. Pirazzini, D. Azarnia Tehran, G. Zanetti, A. Megighian, M. Scorzeto, S. Fillo, C. C. Shone, T. Binz, O. Rossetto, F. Lista, C. Montecucco, Thioredoxin and its reductase are present on synaptic vesicles, and their inhibition prevents the paralysis induced by botulinum neurotoxins. *Cell Rep.* **8**, 1870–1878 (2014).
17. L. K. Koriazova, M. Montal, Translocation of botulinum neurotoxin light chain protease through the heavy chain channel. *Nat. Struct. Biol.* **10**, 13–18 (2003).
18. A. Fischer, M. Montal, Single molecule detection of intermediates during botulinum neurotoxin translocation across membranes. *Proc. Natl. Acad. Sci. U.S.A.* **104**, 10447–10452 (2007).
19. K. H. Lam, Z. Guo, N. Krez, T. Matsui, K. Perry, J. Weisemann, A. Rummel, M. E. Bowen, R. Jin, A viral-fusion-peptide-like molecular switch drives membrane insertion of botulinum neurotoxin A1. *Nat. Commun.* **9**, 5367 (2018).
20. A. Fischer, M. Montal, Crucial role of the disulfide bridge between botulinum neurotoxin light and heavy chains in protease translocation across membranes. *J. Biol. Chem.* **282**, 29604–29611 (2007).
21. G. Schiavo, F. Benfenati, B. Poulain, O. Rossetto, P. Polverino de Laureto, B. R. DasGupta, C. Montecucco, Tetanus and botulinum-B neurotoxins block neurotransmitter release by proteolytic cleavage of synaptobrevin. *Nature* **359**, 832–835 (1992).
22. T. C. Sudhof, J. E. Rothman, Membrane fusion: Grappling with SNARE and SM proteins. *Science* **323**, 474–477 (2009).
23. R. Jahn, R. H. Scheller, SNAREs—Engines for membrane fusion. *Nat. Rev. Mol. Cell Biol.* **7**, 631–643 (2006).
24. E. Kiris, J. C. Burnett, C. D. Kane, S. Bavari, Recent advances in botulinum neurotoxin inhibitor development. *Curr. Top. Med. Chem.* **14**, 2044–2061 (2014).
25. B. Li, N. P. Peet, M. M. Butler, J. C. Burnett, D. T. Moir, T. L. Bowlin, Small molecule inhibitors as countermeasures for botulinum neurotoxin intoxication. *Molecules* **16**, 202–220 (2010).
26. A. Nowakowski, C. Wang, D. B. Powers, P. Amersdorfer, T. J. Smith, V. A. Montgomery, R. Sheridan, R. Blake, L. A. Smith, J. D. Marks, Potent neutralization of botulinum neurotoxin by recombinant oligoclonal antibody. *Proc. Natl. Acad. Sci. U.S.A.* **99**, 11346–11350 (2002).
27. S. S. Arnon, R. Schechter, S. E. Maslanka, N. P. Jewell, C. L. Hatheway, Human botulism immune globulin for the treatment of infant botulism. *N. Engl. J. Med.* **354**, 462–471 (2006).
28. S. Kodihalli, A. Emanuel, T. Takla, Y. Hua, C. Hobbs, R. LeClaire, D. C. O'Donnell, Therapeutic efficacy of equine botulism antitoxin in Rhesus macaques. *PLOS ONE* **12**, e0186892 (2017).
29. P. A. Yu, N. H. Lin, B. E. Mahon, J. Sobel, Y. Yu, R. K. Mody, W. Gu, J. Clements, H. J. Kim, A. K. Rao, Safety and improved clinical outcomes in patients treated with new equine-derived heptavalent botulinum antitoxin. *Clin. Infect. Dis.* **66**, S57–S64 (2017).
30. S. Bade, A. Rummel, C. Reisinger, T. Karnath, G. Ahnert-Hilger, H. Bigalke, T. Binz, Botulinum neurotoxin type D enables cytosolic delivery of enzymatically active cargo proteins to neurones via unfolded translocation intermediates. *J. Neurochem.* **91**, 1461–1472 (2004).

31. M. C. Goodnough, G. Oyler, P. S. Fishman, E. A. Johnson, E. A. Neale, J. E. Keller, W. H. Tepp, M. Clark, S. Hartz, M. Adler, Development of a delivery vehicle for intracellular transport of botulinum neurotoxin antagonists. *FEBS Lett.* **513**, 163–168 (2002).
32. M. Ho, L. H. Chang, M. Pires-Alves, B. Thyagarajan, J. E. Bloom, Z. Gu, K. K. Aberle, S. A. Teymorian, Y. Bannai, S. C. Johnson, J. J. McArdle, B. A. Wilson, Recombinant botulinum neurotoxin A heavy chain-based delivery vehicles for neuronal cell targeting. *Protein Eng. Des. Sel.* **24**, 247–253 (2011).
33. P. A. Band, S. Blais, T. A. Neubert, T. J. Cardozo, K. Ichtchenko, Recombinant derivatives of botulinum neurotoxin A engineered for trafficking studies and neuronal delivery. *Protein Expr. Purif.* **71**, 62–73 (2010).
34. G. Schiavo, O. Rossetto, A. Santucci, B. R. DasGupta, C. Montecucco, Botulinum neurotoxins are zinc proteins. *J. Biol. Chem.* **267**, 23479–23483 (1992).
35. G. Schiavo, B. Poulain, O. Rossetto, F. Benfenati, L. Tauc, C. Montecucco, Tetanus toxin is a zinc protein and its inhibition of neurotransmitter release and protease activity depend on zinc. *EMBO J.* **11**, 3577–3583 (1992).
36. T. Binz, S. Bade, A. Rummel, A. Kollewe, J. Alves, Arg^{362} and Tyr^{365} of the botulinum neurotoxin type a light chain are involved in transition state stabilization. *Biochemistry* **41**, 1717–1723 (2002).
37. E. J. Vazquez-Cintron, P. H. Beske, L. Tenezaca, B. Q. Tran, J. M. Oyler, E. J. Glotfelty, C. A. Angeles, A. Syngkon, J. Mukherjee, S. R. Kalb, P. A. Band, P. M. McNutt, C. B. Shoemaker, K. Ichtchenko, Engineering botulinum neurotoxin C1 as a molecular vehicle for intra-neuronal drug delivery. *Sci. Rep.* **7**, 42923 (2017).
38. S. Pellett, W. H. Tepp, L. H. Stanker, P. A. Band, E. A. Johnson, K. Ichtchenko, Neuronal targeting, internalization, and biological activity of a recombinant atoxic derivative of botulinum neurotoxin A. *Biochem. Biophys. Res. Commun.* **405**, 673–677 (2011).
39. R. P. Webb, Engineering of botulinum neurotoxins for biomedical applications. *Toxins* **10**, 231 (2018).
40. R. P. Webb, T. J. Smith, L. A. Smith, P. M. Wright, R. L. Guernieri, J. L. Brown, J. C. Skerry, Recombinant botulinum neurotoxin Hc subunit (BoNT Hc) and catalytically inactive *Clostridium botulinum* holoproteins (ciBoNT HPs) as vaccine candidates for the prevention of botulism. *Toxins* **9**, 269 (2017).
41. O. Rossetto, C. Montecucco, Tables of toxicity of botulinum and tetanus neurotoxins. *Toxins* **11**, 686 (2019).
42. S. Zhang, G. Masuyer, J. Zhang, Y. Shen, D. Lundin, L. Henriksson, S. I. Miyashita, M. Martinez-Carranza, M. Dong, P. Stenmark, Identification and characterization of a novel botulinum neurotoxin. *Nat. Commun.* **8**, 14130 (2017).
43. C. L. Kuo, G. A. Oyler, C. B. Shoemaker, Accelerated neuronal cell recovery from Botulinum neurotoxin intoxication by targeted ubiquitination. *PLOS ONE* **6**, e20352 (2011).
44. J. M. Tremblay, C. L. Kuo, C. Abeijon, J. Sepulveda, G. Oyler, X. Hu, M. M. Jin, C. B. Shoemaker, Camelid single domain antibodies (VHHs) as neuronal cell intrabody binding agents and inhibitors of Clostridium botulinum neurotoxin (BoNT) proteases. *Toxicon* **56**, 990–998 (2010).
45. M. W. Popp, J. M. Antos, G. M. Grotenbreg, E. Spooner, H. L. Ploegh, Sortagging: A versatile method for protein labeling. *Nat. Chem. Biol.* **3**, 707–708 (2007).
46. J. Blasi, E. R. Chapman, E. Link, T. Binz, S. Yamasaki, P. De Camilli, T. C. Sudhof, H. Niemann, R. Jahn, Botulinum neurotoxin A selectively cleaves the synaptic protein SNAP-25. *Nature* **365**, 160–163 (1993).
47. G. Schiavo, A. Santucci, B. R. Dasgupta, P. P. Mehta, J. Jontes, F. Benfenati, M. C. Wilson, C. Montecucco, Botulinum neurotoxins serotypes A and E cleave SNAP-25 at distinct COOH-terminal peptide bonds. *FEBS Lett.* **335**, 99–103 (1993).
48. M. Dong, F. Yeh, W. H. Tepp, C. Dean, E. A. Johnson, R. Janz, E. R. Chapman, SV2 is the protein receptor for botulinum neurotoxin A. *Science* **312**, 592–596 (2006).
49. S. Mahrhold, A. Rummel, H. Bigalke, B. Davletov, T. Binz, The synaptic vesicle protein 2C mediates the uptake of botulinum neurotoxin A into phrenic nerves. *FEBS Lett.* **580**, 2011–2014 (2006).
50. K. R. Aoki, A comparison of the safety margins of botulinum neurotoxin serotypes A, B, and F in mice. *Toxicon* **39**, 1815–1820 (2001).
51. K. H. Lam, J. M. Tremblay, E. Vazquez-Cintron, K. Perry, C. Ondeck, R. P. Webb, P. M. McNutt, C. B. Shoemaker, R. Jin, Structural insights into rational design of single-domain antibody-based antitoxins against botulinum neurotoxins. *Cell Rep.* **30**, 2526–2539.e6 (2020).
52. S. Zhang, F. Lebreton, M. J. Mansfield, S. I. Miyashita, J. Zhang, J. A. Schwartzman, L. Tao, G. Masuyer, M. Martinez-Carranza, P. Stenmark, M. S. Gilmore, A. C. Doxey, M. Dong, Identification of a botulinum neurotoxin-like toxin in a commensal strain of *Enterococcus faecium*. *Cell Host Microbe* **23**, 169–176.e6 (2018).
53. J. Brunt, A. T. Carter, S. C. Stringer, M. W. Peck, Identification of a novel botulinum neurotoxin gene cluster in *Enterococcus*. *FEBS Lett.* **592**, 310–317 (2018).
54. E. Contreras, G. Masuyer, N. Qureshi, S. Chawla, H. S. Dhillon, H. L. Lee, J. Chen, P. Stenmark, S. S. Gill, A neurotoxin that specifically targets *Anopheles* mosquitoes. *Nat. Commun.* **10**, 2869 (2019).
55. L. Peng, H. Liu, H. Ruan, W. H. Tepp, W. H. Stoothoff, R. H. Brown, E. A. Johnson, W. D. Yao, S. C. Zhang, M. Dong, Cytotoxicity of botulinum neurotoxins reveals a direct role of syntaxin 1 and SNAP-25 in neuron survival. *Nat. Commun.* **4**, 1472 (2013).
56. S. Pellett, W. H. Tepp, J. M. Scherf, E. A. Johnson, Botulinum neurotoxins can enter cultured neurons independent of synaptic vesicle recycling. *PLOS ONE* **10**, e0133737 (2015).
57. Z. Yang, D. Schmidt, W. Liu, S. Li, L. Shi, J. Sheng, K. Chen, H. Yu, J. M. Tremblay, X. Chen, K. H. Piepenbrink, E. J. Sundberg, C. P. Kelly, G. Bai, C. B. Shoemaker, H. Feng, A novel multivalent, single-domain antibody targeting TcdA and TcdB prevents fulminant *Clostridium difficile* infection in mice. *J. Infect. Dis.* **210**, 964–972 (2014).
58. A. R. Schneekloth, M. Pucheault, H. S. Tae, C. M. Crews, Targeted intracellular protein degradation induced by a small molecule: En route to chemical proteomics. *Bioorg. Med. Chem. Lett.* **18**, 5904–5908 (2008).
59. S. L. Paiva, C. M. Crews, Targeted protein degradation: Elements of PROTAC design. *Curr. Opin. Chem. Biol.* **50**, 111–119 (2019).
60. E. Caussinus, O. Kanca, M. Affolter, Fluorescent fusion protein knockout mediated by anti-GFP nanobody. *Nat. Struct. Mol. Biol.* **19**, 117–121 (2011).
61. N. Yamaguchi, T. Colak-Champollion, H. Knaut, zGrad is a nanobody-based degron system that inactivates proteins in zebrafish. *eLife* **8**, e43125 (2019).
62. S. Nagarkar-Jaiswal, P. T. Lee, M. E. Campbell, K. Chen, S. Anguiano-Zarate, M. C. Gutierrez, T. Busby, W. W. Lin, Y. He, K. L. Schulze, B. W. Booth, M. Evans-Holm, K. J. Venken, R. W. Levis, A. C. Spradling, R. A. Hoskins, H. J. Bellen, A library of MiMICs allows tagging of genes and reversible, spatial and temporal knockdown of proteins in Drosophila. *eLife* **4**, e05338 (2015).
63. S. Wang, N. H. Tang, P. Lara-Gonzalez, Z. Zhao, D. K. Cheerambathur, B. Prevo, A. D. Chisholm, A. Desai, K. Oegema, A toolkit for GFP-mediated tissue-specific protein degradation in *C. elegans*. *Development* **144**, 2694–2701 (2017).
64. Y. J. Shin, S. K. Park, Y. J. Jung, Y. N. Kim, K. S. Kim, O. K. Park, S. H. Kwon, S. H. Jeon, A. Trinh, S. E. Fraser, Y. Kee, B. J. Hwang, Nanobody-targeted E3-ubiquitin ligase complex degrades nuclear proteins. *Sci. Rep.* **5**, 14269 (2015).
65. C. Chen, A. Przedpelski, W. H. Tepp, S. Pellett, E. A. Johnson, J. T. Barbieri, Heat-labile enterotoxin IIa, a platform to deliver heterologous proteins into neurons. *mBio* **6**, e00734 (2015).

Acknowledgments: We thank members of the Dong laboratory for discussion and M. Galbreath and K. Hullahalli for assistance in protein purification and molecular cloning. **Funding:** This study was supported by grants from NIH (R01NS080833, R01AI132387, R01AI139087, and R21NS106159 to M.D.; U54AI057159, R21AI088489, and R01AI093467 to C.B.S.) and Intelligence Advanced Research Projects Activity (IARPA, grant number W911NF-17-2-0089 to M.D.). We also acknowledge support from the NIH-funded Harvard Digestive Disease Center (P30DK034854) and Boston Children's Hospital Intellectual and Developmental Disabilities Research Center (P30HD18655). M.D. holds the Investigator in the Pathogenesis of Infectious Disease award from the Burroughs Wellcome Fund. **Author contributions:** S.-I.M., C.B.S., and M.D. initiated the project. S.-I.M. and M.D. designed all experiments. S.-I.M. carried out all experiments. J.Z. helped with animal experiments. S.Z. purified SV2C-L4 and VAMP2 protein. C.B.S. provided VHH sequences. S.-I.M. and M.D. wrote the manuscript. **Competing interests:** Boston Children's Hospital has filed a provisional patent application (catalytically inactive botulinum neurotoxin–like toxins and uses thereof, #US62/835,151) on the chimeric toxin–based delivery technology described here, with S.-I.M. and M.D. as coinventors. **Data and materials availability:** All data associated with this study are present in the paper or the Supplementary Materials. All materials created in this study are available with material transfer agreements approved by Boston Children's Hospital to any researcher for purposes of reproducing or extending the analysis.

Submitted 6 September 2019
Accepted 1 May 2020
Published 6 January 2021
10.1126/scitranslmed.aaz4197

Citation: S.-I. Miyashita, J. Zhang, S. Zhang, C. B. Shoemaker, M. Dong, Delivery of single-domain antibodies into neurons using a chimeric toxin–based platform is therapeutic in mouse models of botulism. *Sci. Transl. Med.* **13**, eaaz4197 (2021).

Science Translational Medicine

Delivery of single-domain antibodies into neurons using a chimeric toxin–based platform is therapeutic in mouse models of botulism

Shin-Ichiro Miyashita, Jie Zhang, Sicai Zhang, Charles B. Shoemaker and Min Dong

Sci Transl Med **13**, eaaz4197.
DOI: 10.1126/scitranslmed.aaz4197

Nontoxic botulinum for drug delivery

Botulism is a severe and potentially fatal disease characterized by muscle paralysis. The causing agent, botulinum neurotoxins (BoNTs), has the ability to enter motor neurons and to block neurotransmission. In two independent studies, Miyashita *et al*. and McNutt *et al*. used nontoxic derivative of BoNT to deliver therapeutic antibodies against BoNTs in neurons. Miyashita *et al*. targeted BoNT/A and BoNT/B and reported therapeutic effects in mice. Using a similar approach targeting BoNT/A, McNutt *et al*. increased survival after lethal challenge in mice, guinea pigs, and monkeys. This approach provided a safe and effective treatment against BoNT intoxication and could be exploited for targeting other intracellular proteins in neurons.